After-Effect of Perceived Regularity

Marouane Ouhnana[1], Jason Bell[2], Joshua A. Solomon[3], Frederick A. A. Kingdom[1]

[1]McGill Vision Research Unit, McGill University, Montreal, Quebec, Canada, email: marouane.ouhnana@mail.mcgill.ca

[2]Research School of Psychology, The Australian National University, Canberra, Australia

[3]Optometry Division, Applied Vision Research Centre, City University London, UK

Abstract

Regularity is a ubiquitous feature of the visual world. We demonstrate that regularity is an adaptable visual dimension: the perceived regularity of a pattern is reduced following adaptation to a pattern with a similar or greater degree of regularity. Our stimuli consisted of 7 by 7 element arrays arranged on square grids presented in a circular aperture. The position of each element was randomly jittered from its baseline position by an amount that determined its degree of irregularity. The elements of the pattern consisted of dark Gaussian blobs (GBs), difference of Gaussians (DOGs) or random binary patterns (RBPs). Observers adapted for 60 seconds to either a single or to a pair of patterns with particular regularities, and the perceived regularities of subsequently presented test patterns were measured using a conventional staircase matching procedure. We found that the Regularity After-Effect (RAE) was unidirectional: adaptation only caused test patterns to appear less regular. We also found that RAEs transferred from GB adaptors to both DOG and RBP test patterns and from DOG and RBP adaptors to GB patterns. We suggest that regularity is coded by the peakedness in the distribution of spatial-frequency channel responses across scale, and that the RAE is a result of a flattening of this distribution by adaptation. Thus the RAE may be a phenomenological consequence of contrast normalization, and an example of norm-based coding where irregularity is the norm.

Keywords: regularity, after-effect, adaptation, spatial vision

Introduction

A regular pattern is a pattern with repeating features. Regularity, and its inverse, irregularity, may be a considered a physical *dimension*, in that some patterns are more regular (or less irregular) than others. Patterns with a degree of regularity, i.e. with a degree of repetition, are ubiquitous in our visual world, in both natural and man-made environments. In biological organisms, regularity results from specific developmental growth processes, for example the repeated substructures in an animal's pelt (Mandelbrot, 1982). Abnormalities in such repetitions may be seen as flaws in an otherwise normal biologically-planned growth process. In man-made structures, one finds that aesthetics, manufacturing ease and functionality underpin regularity. For example, repetition of elements is often the most prominent feature in the definition of an architectural style. In vision, regularity is a pop-out feature, as shown in Fig. 1, and might reasonably be considered a "Gestalt", that is a class of visual pattern with which our visual system synergizes, similar to other Gestalts such as good continuation, mirror-symmetry, common fate etc. (Wertheimer, 1938). One might therefore expect that the human visual system is especially attuned to regularity, which would facilitate the efficient coding of an important class of visual information (Attneave, 1954; Lee & Yuille, 2007).

Figure 1 approximately here

To our knowledge only one study has explicitly sought to understand the mechanisms mediating the perception of regularity. Morgan, Mareschal, and

Solomon (2012) studied sensitivity to regularity in grids, circles and lines of regularly spaced dots. The position of each dot in the pattern could be randomly perturbed from its notional, regular position, and thresholds were measured for detecting this perturbation as a function of the baseline, or 'pedestal' perturbation. From the pattern of results Morgan et al. concluded that the visual system possesses an internal template of a regular pattern, and that perceived departures from regularity occur when the amount of physical perturbation exceeds an equivalent internal noise level. The suggestion of an internal template for regularity may be taken to imply the presence of a dedicated mechanism for detecting departures from regularity.

Adaptation paradigms have long been used in vision research to identify mechanisms selective for different stimulus attributes (reviewed by Webster, 2011). If prolonged fixation of a stimulus results in a change in a behavioral measure on a particular stimulus attribute, this is taken to imply the existence of a mechanism specific to that adapted attribute. In this communication, we describe a series of psychophysical experiments, using normal human observers as test subjects, aimed at determining whether regularity is an adaptable visual feature, as evidenced by whether it produces an after-effect. Our stimuli consist of arrays of micro-patterns (blurred dots, bulls-eye patterns, and random binary patterns), whose positions are determined by specified random perturbations from notional grid

positions – see Fig. 2. We find evidence that regularity does indeed produce an after-effect, and go on to determine a number of its perceptual properties.

One of the perceptual properties we have investigated concerns whether the after-effect occurs in patterns whose elements are contrast-defined rather than luminance-defined. The luminance-defined elements we use are the Gaussian blobs shown in Fig. 1 and on the left side of Fig. 2, whereas the contrast-defined elements are the random binary pattern elements shown on the bottom right half of Fig. 2. Traditionally, visual mechanisms sensitive to luminance variations are termed '1st-order' whereas those sensitive to contrast variations are termed '2nd-order' (Graham, 2011). While these terms characterize the mechanisms involved in detecting the individual elements in our patterns, the encoding of their *arrangement*, which is of primary interest here, likely involves mechanisms that are at least one order higher. Thus on the one hand neurophysiological and psychophysical evidence suggests that distinct mechanisms detect the two types of element in early vision (e.g. Nishida, Ledgeway, and Edwards, 1997; Schofield and Georgeson, 1999, Baker & Mareschal, 2001; reviewed by Baker, 1999 and Graham, 2011), other evidence suggests that in the higher stages of vision mechanisms exist that respond to both types of stimuli (reviewed by Baker, 1999). What is the situation for the encoding of regularity?

Figure 2 approximately here

General Methods

Observers

Seven observers participated in the project, three of the authors (MO, JB, & FK) and four additional observers (AK, MK, CD and DW) who were naïve as to the experimental aims. All participants had normal or corrected-to-normal visual acuity. Participation was voluntary and was not financially compensated. Written consent was obtained from all test subjects, and all experimental protocols were approved by the McGill University Research Ethics Board.

Apparatus

The stimuli were created using Matlab version 7.8 and generated using either a Cambridge Research Systems (CRS) Visage or VSG2/5 video-graphics card, and displayed on a Sony FD Trinitron GDM-F500 monitor. The resolution of the monitor was set to 1024 x 768 with a refresh rate of 100 Hz. The monitor's Z-nonlinearity was corrected using look-up tables following calibration with an Optical OP200-E photometer. The mean luminance of the monitor was 33.9 cd/m^2.

Stimuli

Stimuli were constructed from three types of element: Gaussian blobs (GBs), difference-of-Gaussians (DOGs), and random binary patterns (RBPs). The GBs were 'dark' and orientationally isotropic, i.e. circularly-symmetric, according to the formula:

$$L(x,y) = L_{mean}\left[1 + C\frac{-1}{2\pi\sigma^2}\exp\left(-\frac{x^2+y^2}{2\sigma^2}\right)\right]$$

Eqn. 1

where x and y are Cartesian coordinates, L_{mean} is the background luminance, C contrast (amplitude/mean), and σ the standard deviation (SD). Unless otherwise stated C was set to 1 to give maximum 'dark' contrast and σ was set to either 3.8 or 7.7 arcmin at the viewing distance of 100 cm.

The DOGs were 'dark-on-center' and isotropic, generated according to the formula:

$$L(x,y) = L_{mean}\left(1 + C\left[\frac{-1}{2\pi\sigma^2}\exp\left(-\frac{x^2+y^2}{2\sigma^2}\right) - \frac{-1}{2\pi R^2\sigma^2}\exp\left(-\frac{x^2+y^2}{2R^2\sigma^2}\right)\right]\right)$$

Eqn. 2

with R=1.6 and σ 3.8 arcmin.

The RBPs were generated by the product of an array of randomly allocated binary values from a rectangular distribution (0 & 1) and a Gaussian (Eqn. 1) with SD of 7.7 arcmin.

Adaptor and test stimuli

The stimuli consisted of 7x7 grids of elements windowed through an aperture of diameter of 4 deg, softened by a Gaussian edge with a standard deviation of 5 arcmins. The position of each element was randomly selected from

two rectangular distributions, one horizontal and the other vertical, with ranges centered on the notional grid position. The elements were displayed on a mid-grey background of 33.9 cd/m^2. For the adapting stimuli, depending on whether a single- or dual-adaptor paradigm was employed (see below), the stimuli were presented three degrees above and/or below a fixation dot located in the center of the screen. In the single-adaptor condition, the adaptor element jitter was set to 0, 5, 10, 15, 20, 25, and 30 arcmin. For the dual-adaptor conditions, one of the adaptors was set to a jitter range of 6, while the other at 24 arcmin. The test-patterns consisted of a pair of stimuli presented above and below a fixation dot.

Procedure

Participants viewed the display in a well-lit room and were instructed to fix their gaze on the fixation dot for the entire session. Each session began with an initial adaptation period of 60s. During adaptation the overall position of each stimulus pattern was jittered every 500ms over a range of 20 arcmin in a random direction, and the within-stimulus element positions were refreshed by re-jittering them according to their specified degree of regularity. Both types of jitter helped to minimize the build-up of after-images. Each test cycle began with a 500 ms blank interval with a fixation dot, followed by a 500 ms test pair, then another 500 ms blank interval and finally top-up adaptation of 2.5s. The onset of the test patterns was signaled by a tone.

A staircase procedure was used to determine the magnitude of the Regularity After-Effect (RAE), defined as either the difference or the ratio (depending on the experiment) of the regularity of the two tests, or the test and comparison patterns, at the point-of-subjective equality (PSE). The exact procedure depended on whether a single or dual-adaptor was employed (see Fig. 3) and whether the staircase adjusted the difference or the ratio of the test-pair regularities.

Single-adaptor procedure

For the single adaptor method, the test stimulus was located in the same position as the adaptor and was fixed at 15 arcmin jitter, while the comparison stimulus was positioned on the other hemi-field (above or below) of the fixation dot and whose regularity was determined in each trial by the staircase procedure. For the 'difference' adjustments, the initial regularity of the comparison was randomly selected from the range 10 to 20 arcmin jitter, while for the 'ratio' adjustments the initial regularity of the comparison pattern was randomly selected from the range 10 to 22.5 arcmin jitter. On each trial during the test period, participants indicated via button press whether the upper or lower test pattern was perceived as more regular. Following the response, the computer modified the regularity of the comparison pattern in a direction towards the PSE, either by adding/subtracting the jitter difference, or by multiplying/dividing the jitter ratio. If no response was made in this window, then the test patterns were unchanged on the subsequent trial.

Figure 3 approximately here

After 25 trials the session was stopped, and the size of the RAE calculated as the mean difference, or geometric mean ratio of the jitter differences/ratios over the last 20 trials. For the single-adaptor experiments, eight measurements were taken, four with the single adaptor above, and four below fixation. Eight no-adaptor baseline measures were also obtained, four with the test pattern above and four with the test pattern below fixation.

Dual-adaptor procedure

For the dual-adaptor method there were two adaptors, one above and one below fixation, and two corresponding tests patterns. During the test period the regularities of both test patterns were adjusted by the staircase procedure. For the difference adjustments, the initial regularity of one of the two test patterns was randomly selected from the range 10 to 20 arcmin jitter, while that of the other test pattern was set to its complement such that the mean of the two regularities was 15 arcmin jitter. For the ratio adjustments, the initial regularity of one of the test patterns was randomly selected from the range 10 to 22.5 arcmin jitter, while that of the other test pattern was set to the complement such that the geometric mean regularity of the two test patterns was also 15 arcmin jitter.

During the first 5 trials, the regularity difference between the two test patterns was incremented or decremented by 4 arcmins of jitter, or the regularity ratio of the two test patterns was multiplied or divided by 1.25. For the remaining trials the values were 2 arcmin added/subtracted or 1.1 multiplied/divided. The

session was stopped after 25 trials, and the RAE for that session calculated as the mean difference/ratio over the previous 20 trials.

Eight measurements were taken, four with the more regular pattern above and four below fixation. In addition four measurements were taken in the absence of the adaptors, with all else being equal.

Calculation of the RAE

For both single- and dual-adaptor methods, an overall estimate of the RAE was calculated as follows. For the difference adjustment experiments, the mean of the no-adaptor baseline measures was subtracted from each adaptor-present measure, and the mean and standard errors of these subtractions was calculated across measurements. In the case of the ratio adjustment experiments, the mean of the no-adaptor baseline log PSE ratios was subtracted from each adaptor-present log PSE ratio and the mean and standard error of the subtractions was calculated across measurements.

Experiments

Is there a Regularity After-Effect?

This experiment considered whether regularity is an adaptable feature of the visual system, by examining whether it produces a regularity after-effect, or RAE. The stimuli were made of dark Gaussian blobs (GBs) with an SD of 3.8 arcmin, and the dual-adaptor method was employed.

Fig. 4 shows RAEs for five observers (FK, MO, JB, CD, & AK). The figure plots the jitter-range difference between the upper and lower test patterns at the PSE for each observer after subtracting the baseline PSE and the error bars show 95% confidence limits (i.e. not standard errors). The figure shows that all three subjects exhibited an RAE, since none of the error bars were even close to zero (no RAE). The data from the three observers were collapsed into one data set (d.f. = 5 subjects x 8 measures, - 1 = 39) and a correlated-sample t-test was conducted that revealed that the mean RAE was significantly different than zero $t(39)= 17.86$, $p<0.01$ (two-tailed). The results demonstrate that there is a regularity after-effect.

Figure 4 approximately here

Is the RAE unidirectional or bidirectional?

The above experiment, by virtue of using the dual-adaptor method, does not reveal the directionality of the after-effect. That is, it does not reveal whether 1. the more regular adaptor caused the effect by making the corresponding less regular test pattern appear even less regular, 2. the less regular adaptor caused the effect by making the corresponding more regular test pattern appear even more regular, or 3. both adaptors caused the effect by making the less regular test pattern appear even less regular and the more regular test pattern appear even more regular. If either of the first two possibilities is the case the aftereffect may be deemed unidirectional, whereas if the third possibility is the case the aftereffect may be deemed bidirectional.

The aim of this experiment therefore was to determine whether the RAE is unidirectional or bidirectional. This entailed using the single-adaptor method. Thus only a single adaptor was presented per session, with the test pattern presented in the same location as the adaptor. The 'measuring stick' in the single-adaptor method was the comparison pattern that was presented in the other hemi-field to that of the adaptor/test, and it was the comparison pattern only that was adjusted during the staircase procedure. The test pattern was fixed at an irregularity of 15 arcmin jitter, and adaptor irregularities of 0, 5, 10, 15, 20, 25, and 30 arcmin jitter were employed. The grid elements were similar to those used in the previous experiment.

Fig. 5 shows the resulting RAEs for three observers (MO, JB, & DW). The figure plots the jitter-range difference between the test and comparison patterns at the PSE for each observer (after subtracting the baseline PSE) for each adaptor irregularity. All RAEs were positive, indicating that the test pattern only ever appeared less regular following adaptation, irrespective of whether the adaptor irregularity was greater than, lesser than, or equal to that of the test. Thus the RAE is unidirectional. Moreover, the magnitude of the after-effect appears to decline with adaptor irregularity.

Figure 5 approximately here

Is the RAE due to local positional-adaption?

Positional adaptation produces a repulsive shift in subsequently presented elements away from their physical locations (Whitaker, McGraw, and Levi, 1997). For example, following adaptation to a three-element stimulus whose middle element is slightly offset, the middle element of a subsequent group of three aligned elements appears slightly offset in the opposite direction (Hess & Doshi, 1995; Yeh et al., 1991). In our attempt to prevent the build-up of after-images during adaptation, we jittered the adaptor patterns as a whole. However, it is possible that the amount of jitter was insufficient to rule-out adaptation to element modal-positions. The aim of this experiment was to assess whether local positional-adaptation underlies the observed RAE.

Using Gaussian blobs (GBs) with an SD of 3.8 arcmin and the dual-adaptor method, two adaptor global jitter conditions were tested: 20 arcmin and 40 arcmin. Since the peak-to-peak inter-element distance of the perfectly regular pattern was 41 arcmin, 20 arcmin of global jitter means that the smallest possible separation between corresponding elements in subsequent adaptor presentations is 21 arcmin. This means that there will still be regions of the retinal image that would never be stimulated by the perfectly regular Gaussian blobs during adaptation. Doubling the amount of global jitter to 41 arcmin eliminates this unadapted space, thus ensuring that every test element is subject to adaptation from elements positioned equally (on average) at all points around it, thus minimizing the effects of local positional adaptation. Fig. 6 shows RAEs for two observers (MO & JB). The

figure plots the jitter-range difference between the upper and lower test patterns at the PSE for each observer after subtracting the baseline PSE, for each of the global adaptor jitter values. The figure shows that both subjects exhibited equal amounts of RAE regardless of global adaptor jitter amount. The data from the two observers were collapsed into two data sets corresponding to the standard procedure and the adjusted adaptor global jitter value. A correlated-sample t-test was conducted and revealed that the mean differences were not significantly different than zero $t(11)= 0.5723$, $p>0.05$ (two-tailed). The results demonstrate that positional adaptation does not underlie the RAE. As a conservative approach all subsequently presented experiments used the global jitter value of 40 arcmin.

Figure 6 approximately here

Is there an RAE for contrast-defined elements?

The purpose of this experiment was to assess whether the RAE occurs with contrast-defined and not luminance-defined elements, and if it does, whether the same mechanism is involved for both. We employed two types of contrast-defined element: Difference-of-Gaussian (DOG) and random binary pattern (RBP) elements.

RAEs were measured for all three types of element when the same element was used in both adaptor and test, termed the congruent condition, as well as a condition in which adaptor and test were of a different type, termed the incongruent condition. Use of both congruent and incongruent conditions enabled us to

measure the amount of transfer of the RAE from one type of element to the other. The experiment was divided into two parts: 1. RAEs measured using GBs and DOGs, both with an SD of 3.8 arcmin and a contrast of 33% and 2. RAEs using GBs and RBPs, both with an SD of 7.7 arcmin and presented at full contrast.

We used larger SDs and higher contrasts in the second part of the experiment as the RBP elements were less salient than the other two elements at small SDs. The dual-adaptor method was employed with a total of 4 adaptor-test combinations in each part of the experiment. In part 1 we tested: adaptor GB test GB; adaptor GB test DOG; adaptor DOG test DOG; adaptor DOG test GB. In part 2 we tested: adaptor GB test GB; adaptor GB test RBP; adaptor RBP test RBP; adaptor RBP test GB. No-adaptor baselines for GBs, DOGs and RBPs were also measured.

Results are shown in Fig. 7 for part 1 (GBs and DOGs) and Fig. 8 for part 2 (GBs and RBPs). The data for both parts of the experiment were collapsed into two groups: adaptor-test congruent, and adaptor-test incongruent. For the data in Fig. 7 a two sample dependent t-test was conducted and revealed that the mean RAE for the congruent and incongruent adaptor-test pairings was not significantly different $t(47)= 0.9372$, $p>0.05$ (two-tailed). For the data in Fig. 8 the two sample dependent t-test also revealed no significant difference in the mean RAE for the congruent and incongruent adaptor-test pairings $t(47)= 1.295$, $p>0.05$ (two-tailed).

These results are not consistent with the idea that the RAE is mediated by separate mechanisms for luminance-defined and contrast-defined elements.

Figure 7 approximately here

Figure 8 approximately here

Discussion

The following summarizes the main findings of this study:

1. An after-effect of perceived regularity, or RAE, can be induced in grids of Gaussian Blob (GB), Difference-of-Gaussian (DOG) and random-binary-pattern (RBP) elements.

2. The RAE is a unidirectional after-effect, that is adapting to pattern regularity only ever makes a subsequent pattern appear less regular.

3. Positional-adaptation is not sufficient to explain the RAE.

4. The RAE transfers from GB to DOG elements and vice-versa, and from GB to RBP elements, and vice-versa.

A new after-effect of perceived regularity

We have demonstrated a new after-effect, the regularity after-effect, or RAE. The RAE is experienced as an increase in the departure from the notional positions of elements on a grid.

Relationship to other spatial after-effects

Other unidirectional after-effects have been found. Adaptation to contrast only ever makes a subsequently presented pattern appear to have less contrast (Georgeson, 1985) and adaptation to density only ever makes a subsequently presented pattern look less dense (Durgin and Huk, 1997). On the other hand, the tilt after-effect and spatial-frequency after-effects are bi-directional. Adaptation to an oriented line always causes a line of slightly different orientation to appear oriented in a direction away from that of the adaptor orientation (Gibson and Radner, 1937), and adaptation to a figure of given size always causes a figure of slightly different size (whether bigger or smaller than the adaptor) to appear shifted away from that of the adaptor size (Sutherland, 1954). It has been suggested that bi-directionality in after-effects is supportive of the idea that the dimension of interest is processed by multiple channels each tuned to a specific range of the dimension (Webster, 2011). Thus our findings provide no support for the idea that regularity is coded via multiple channels each selective to a particular range of irregularity.

An important difference with some other uni-directional after-effects concerns the relationship between adaptor and test regularities and the magnitude of the after-effect. In his study of contrast adaptation using sine-wave gratings, Georgeson (1985) found that significant reductions in apparent contrast following adaptation only occurred when the test was lower in contrast than the adaptor. In

the present study, as is clear from Fig. 5, the apparent regularity of a test pattern is reduced by adaptors both greater *and* smaller in regularity than the test, though the amount of reduction is smaller for the latter. This property of the RAE is a feature of norm-based coding (Webster, 2011; H. Dennett, personal communication), where the effect of adaptation is always to shift perception towards the norm. For example with blur adaptation, adaptation to either a blurred or to a sharpened image results in the image appearing more focused, or 'neutral': in this case the norm is 'focused' (Elliott, Georgeson, & Webster, 2011). For the RAE, it is indeed a consequence of norm-based coding, then the norm that it reveals is 'irregular'. This might at first seem counter-intuitive, but as Fig. 1 demonstrates, regularity is a pop-out feature and therefore it is irregularity, not regularity, that would seem to be the norm in vision. The explanation of the RAE that we later provide is consistent with the idea that irregularity is treated as a norm by vision.

Regularity coding with luminance-defined and contrast-defined elements

The data are not consistent with the idea that the RAE is mediated by mechanisms that separately process luminance-defined and contrast-defined elements. In one of their texture density adaptation experiments, Durgin and Huk (1997) used different sizes of Gaussian blobs, as well as balanced elements (as in the DOG elements used here) to explore the spatial-frequency selectivity of texture density coding. They found that the direction of the after-effect was unaffected by element type; however the aftereffect was reduced if the adaptor and test elements

were different. Durgin & Huk (1997) concluded that texture density coding was specific to element type at an early stage of visual processing, but that information from different element types was pooled at a later stage. The data presented here for regularity is inconsistent with the first but not the second of Durgin & Huk's conclusions.

Explanation of the RAE

Here we offer an explanation of the RAE that is consistent not only with our results but with known physiology, and also with the concept of norm-based coding. The explanation is motivated in part by a simple demonstration shown in Fig. 9, which shows the result of swapping the Fourier amplitude and phase spectra of a perfectly regular and an irregular pattern with 30 arcmin jitter. The figure reveals that, at least in our stimuli, regularity is predominantly carried by the amplitude not the phase spectrum. The demonstration is especially pertinent when one considers that with images of natural scenes the opposite is found, i.e. the recognizable structure of the scene is carried in the phase not amplitude spectrum (Oppenheim & Lim, 1981; Piotrowski & Campbell, 1982).

Figure 9 approximately here

The revealed role of the amplitude spectrum in representing regularity lends itself to an explanation of the RAE in which the effect of adaptation is to alter the relationship among the response amplitudes of visual filters that respond to the

stimuli. A schematic of our proposed explanation is shown in Fig. 10 as it applies to the GB element patterns, and its extension to RBP element patterns is part-illustrated in Fig. 11.

The basis of the idea in Fig. 10 is that the grid pattern is processed by a standard Filter-Rectify-Filter cascade (Graham, 2011), consisting of a bank of oriented '1st-stage' filters tuned to a range of spatial frequencies, whose outputs are first rectified by squaring (or by a similar nonlinearity) to produce energy responses, which are then summed across the image by a '2nd-stage' filter. To obtain a measure of the output of the putative 2nd-stage in response to our stimuli we conducted the following simulation. Vertically-oriented 1st-stage Gabor filters were defined by the formula:

$$\mathrm{F(x, y,)} = \exp\left(-\frac{x^2 + y^2}{2\sigma^2}\right)\cos\left(2\pi f x\right)$$

where σ is the standard deviation of the Gaussian envelope and *f* the spatial frequency of the underlying sinusoidal modulation. These two parameters were related to produce filters with a constant bandwidth of 1.5 octaves. Gabor filters with σs ranging from 1 arcmin to the full width of the regularity pattern were convolved with two types of pattern, one completely regular (0 arcmin jitter) and one irregular with an element jitter of 30 arcmin. The r.m.s. (root mean square) response for each filter across the convolution image was normalized to equate

responses to matching Gabor stimuli across scale by dividing its response by σ^2. Convolutions were conducted in Matlab.

The plot in Fig. 10c shows the normalized r.m.s. responses for both pattern regularities as a function of the logarithm of filter frequency *f* in cycles per image. For both plots there is a local response peak at *f* = 1.2 log cycles per image; this peak is for the filter whose excitatory receptive-field center is matched in size to that of a single element. The fully regular pattern (blue) plot however also produces a primary peak at around 0.85 log cycles per image where the filter receptive field is matched to the duty cycle of the pattern as a whole. No such primary peak however is observed for the irregular pattern (red) whose response is much reduced at this point.

Figure 10 approximately here

We suggest that the regularity of the pattern is encoded via some measure of the peakedness of the population distribution of SF-tuned filter energy responses across receptive-field size. We suppose that the effect of adaptation is to make the responses across scale more equal, and because the response distribution to the adaptor has a bandpass characteristic, this will have the effect of flattening the response distribution. Thus after adaptation, any test pattern will be encoded as less regular than otherwise because its response distribution across scale will be flatter than otherwise.

If this explanation is correct, the RAE may be considered as a consequence of the canonical process of contrast normalization, one of whose effects is to balance the responses of visual channels across orientation and/or scale (reviewed by Carrandini & Heeger, 2011; see also Blakeslee & McCourt, 1999, Dakin & Bex, 2003, and Robinson, Hammon & de Sa, 2007, for other illusory phenomena explained by contrast normalization).

Fig. 11 shows how the scheme can be extended to deal with the RBP element patterns, by including an additional front-end stage of filtering and rectification to enable the SF-tuned filters to detect the RBP elements that fall within its receptive field. We suggest that the final spatial pooling stage is common to patterns made from either Gaussian blobs or random binary elements.

The 2nd-stage filter for the Gaussian blob patterns and the 3rd stage filter for the RBP element patterns in our scheme is a lowpass filter because our stimuli are uniform in their regularity. In traditional FRF models of texture segregation, the 2nd-stage filter is typically bandpass, because it is designed to detect changes in the texture dimension of interest within the stimulus (Graham, 2011). Indeed if the principle behind our explanation is correct, effortless segregation of the two regions in Fig. 1 is probably mediated by a bandpass not lowpass 2nd-stage filter, in line with other texture-segregation models.

Figure 11 approximately here

This explanation for the RAE is consistent with the uni-directionality of the RAE, because the effect of adaptation is only ever to flatten the population response, causing all test patterns to appear less regular than otherwise. It also explains why adaptation to a pattern of given regularity will make even a more regular test pattern appear less regular (see Fig. 5). This is because it is the *shape* of the response distribution across scale that determines regularity irrespective of the magnitudes of the set of channel responses. In other words it should not matter if some of the channels respond more to the test than to the adaptor: the flattening will always carry over to the test. With simple contrast adaptation, which only has a significant effect on tests that are lower in contrast, the relative magnitudes of adaptor and test are what clearly matter, not the shape of the response distribution across scale. Our explanation of the RAE is also in keeping with the idea that the visual system treats irregularity as a norm, in which the norm is a more-or-less even distribution of filter responses across scale (e.g. Dakin & Bex, 2003).

H. Dennett (personal communication) has suggested that regularity might be encoded by the response *magnitude* of neurons in the high stages of vision, as is believed to be the case for certain other high-level functions such as shape (De Baene, Premereur, & Vogels, 2007; Kayaert, Biederman, Op de Beeck, & Vogels, 2005; Pasupathy & Connor, 2001), and face (Freiwald, Tsao, & Livingstone, 2009) processing. Adaptation would have the effect of reducing the sensitivity of these

neurons, shifting their responses to “less regular”. If such neurons exist, perhaps it is they that encode the peakedness of the population distribution of pooled energy responses, which we have suggested underpins the encoding of regularity (Figs. 10 and 11). This explanation of the RAE shifts the proposed site of adaptation to neurons that code regularity directly via response magnitude, away from the earlier stages that provide their input. We accept this possibility; indeed it is likely that adaptation occurs at multiple sites throughout the regularity-processing chain.

The claim that regularity is an adaptable feature in human vision might be taken to imply that the RAE should be invariant to transformations in both scale and orientation, that is undiminished when adaptor and test differ along one or other of these dimensions. Consider in this regard some other well-known spatial aftereffects. The tilt aftereffect, in which adaptation to an oriented line or grating causes a repulsive shift in the perceived orientation of a line/grating of slightly different orientation, is universally believed to implicate orientation as an adaptable feature, yet is selective for spatial frequency (Ware & Mitchell, 1974), as is also the related color-contingent tilt aftereffect (Held, Shattuck-Hufnagel & Moskowitz, 1982). Another well-known aftereffect is the spatial-frequency aftereffect, in which adaptation to a grating of a given spatial-frequency causes a repulsive shift in the perceived spatial-frequency of grating with a slightly different spatial-frequency. This aftereffect implicates spatial-frequency as an adaptable feature, yet it too is selective, this time for grating orientation (Blakemore, Nachmias & Sutton, 1970).

These findings imply that adaptability along one spatial dimension is often accompanied by specificity along other spatial dimensions. Therefore the validity of the claim that regularity is an adaptable feature is not contingent on the RAE being agnostic to transformations in scale and/or orientation.

Does our explanation for the RAE however lead to predictions concerning the specificity of the RAE to scale and orientation? Since the hypothesized gain reduction that is the basis of our explanation is maximal for spatial mechanisms tuned to both the duty-cycle and orientation of the pattern (see Fig. 10), then indeed we would expect the RAE to show a significant degree of selectivity to both the duty-cycle and overall orientation of the patterns.

Finally, as we noted in the Introduction, Morgan et al. (2012) suggested that the visual system forms an internal representation of a regular template, be it a square grid, notional circle or other. Our model does not preclude the existence of regularity templates for *performance* tasks such as threshold discrimination, but does suggest that for *appearance* tasks regularity might be encoded instead via the shape of a channel response distribution.

Conclusion

In this communication we have demonstrated that regularity is an adaptable feature in human vision. We have demonstrated a novel unidirectional after-effect of perceived regularity, the RAE, in which adaptation to a pattern of given regularity

causes a subsequently presented pattern to appear less regular. We have presented evidence that the RAE is mediated by second-order not first-order mechanisms, and we have proposed a model of the RAE in which regularity is encoded by the degree of peakedness in the response distribution of oriented second-order filter responses across scale.

Figure captions

Fig. 1. Texture segregation based on regularity. The inner region of the texture contains equidistant elements, while the outer region contains elements with added perturbation to their notional positions. The central target 'pops-out'.

Fig. 2. Examples of adaptor pairs similar to the ones used in the experiments. All patterns consist of a 7x7 grid of elements windowed by an aperture. In all panels, the top adaptor is a regular pattern with a jitter of 6 arcmin, while the lower adaptor is a less regular pattern with a jitter of 24 arcmin. Starting clockwise from top-left the elements are Gaussian blobs, Difference of Gaussians, large Gaussian blobs, and Random Binary Patterns.

Fig. 3. Top, dual-adaptor and bottom, single-adaptor methods. Following adaptation, the regularities of both test patterns in the upper right panel are adjusted during the staircase procedure. In the bottom right panel the upper pattern is the test and is fixed in regularity, while the lower pattern is the comparison pattern whose regularity is adjusted during the staircase procedure.

Fig. 4. Regularity after-effect for five observers revealed using the dual-adaptor method. The figure shows the difference in test regularities at the PSE following adaptation minus the no-adaptation baseline PSEs and the error bars show 95% confidence intervals.

Fig. 5. Directionality of the RAE determined using the single-adaptor method. The RAE is plotted as a function of the irregularity of the adaptor, for a fixed test irregularity of 15 arcmin (shown by the grey arrow). Error bars are standard errors. Adaptation only ever causes the test to appear less regular, i.e. the RAE is uni-directional.

Fig. 6. Regularity after-effect for two observers for two adaptor global jitter values. Dual-adaptor method. The figure shows the difference in test regularities at the PSE following adaptation minus the no-adaptation baseline PSEs. Error bars are standard errors.

Fig. 7. Top: RAEs are plotted as a function of the combination of adaptor and test element type. Gaus. = Gaussian blob elements; DOG = Difference-of-Gaussian elements. Bottom: Congruent refers to the combination of adaptor and test in this case collapsing Adaptor Gaus. Test Gaus. and Adaptor DOG and Test Dog, while incongruent refers to Adaptor Gaus. Test DOG and Adaptor DOG and Test Gaus. Error bars are standard errors.

Fig. 8. Top: RAEs as a function of adaptor and test element type. Gaus. = Gaussian blob elements; RBP=Random Binary Pattern elements. Bottom: Congruent refers to the combination of adaptor and test in this case collapsing Adaptor Gaus. Test Gaus. and Adaptor RBP and Test RBP, while incongruent refers to Adaptor Gaus. Test RBP and Adaptor RBP and Test Gaus. Error bars are standard errors.

Fig. 9. The effect of swapping the Fourier amplitudes and phases of a perfectly regular (top left) and highly irregular patterns (top right). Regularity is preserved in the pattern generated from the amplitude spectrum of the regular and phase spectrum of the irregular (bottom left) pattern, not the other way round (bottom right), showing that regularity in our patterns is carried by the amplitude not phase spectrum.

Fig. 10. Explanation of the RAE involving a standard Filter-Rectify-Filter mechanism. Regularity is encoded via the peakedness of the population of spatially pooled energy responses of narrowband spatial-frequency filters. a) regular pattern made up of Gaussian elements with one scale of model Gabor 1^{st}-stage filter. The filter outputs are squared and pooled across the image by a circular filter. b) irregular pattern with same 1^{st}-stage filter c) Pooled energy responses as a function of the scale of the 1^{st}-stage filter, for the regular (blue) and irregular (red) patterns.

Fig. 11. RAE model for patterns made from random binary pattern (RBP) elements

Acknowledgements

The authors thank Dr. Curtis L. Baker Jr, Dr. Aaron P. Johnson, and Dr. Michael J. Morgan for their helpful comments. This research was supported by an Australian Research Council (ARC) Discovery Project Grant (DP110101511) given to J.B., an Engineering and Physical Sciences Research Council (EPSRC) Grant (EP/H033955) given to J.A.S., and a Natural Sciences and Engineering Research Council of Canada (NSERC) Grant (OGP01217130) given to F.K.

Commercial relationships: none.

Corresponding author: Marouane Ouhnana

Email: marouane.ouhnana@mail.mcgill.ca

Address: McGill Vision Research Unit, McGill University, 687 Pine Av. W., Montreal, Quebec, Canada, H3A 1A1

References

Attneave, F. (1954). Some informational aspects of visual perception. Psychological Review, 61(3), 183-193. doi: 10.1037/h0054663

Baker C. L. Jr (1999). Central neural mechanisms for detecting second-order motion. Current Opinion in Neurobiology, 9, 461-466.

Baker C. L. Jr, Mareschal I. (2001). Processing of second-order stimuli in the visual cortex. Progress in Brain Research, 134, 1-21.

Blakemore, C., Nachmias, J. & Sutton, P. (1970) The perceived spatial frequency shift: evidence for frequency-selective neurones in the human brain. *J. Physiol*., 210, 727-750.

Blakeslee, B., & McCourt, M. E. (1999). A multiscale spatial filtering account of the White effect, simultaneous brightness contrast and grating induction. Vision Research, 39, 4361–4377.

Carandini, M. & Heeger, D. J. (2011). Normalization as a canonical neural computation. Nature Reviews Neuroscience, 13(1), 51-62.

Dakin, S. C., & Bex, P. J. (2003). Natural image statistics mediate brightness 'filling-in'. Proceedings of the Royal Society of London Series B – Biological Sciences, 270, 2341–2348.

De Baene, W., Premereur, E., & Vogels, R. (2007). Properties of shape tuning of macaque inferior temporal neurons examined using rapid serial visual presentation.

Durgin, F. H., Huk A. C. (1997). Texture density aftereffects in the perception of artificial and natural textures. Vision Research, 37(23), 3273-3282.

Elliott, S. L., Georgeson, M. A., & Webster, M. A. (2011). Response normalization and blur adaptation: Data and multi-scale model. Journal of Vision, 11(2):7,1–18.

Freiwald, W. A., Tsao, D. Y., & Livingstone, M. S. (2009). A face feature space in the macaque temporal lobe. Nature Neuroscience, 12(9), 1187-1196. doi: 10.1038/nn.2363

Georgeson M. A. (1985). The effect of spatial adaptation on perceived contrast. Spatial Vision, 1(2), 103-112.

Gheorghiu E., Kingdom F. A. A., Sull M., Wells S., (2009). Curvature coding in illusory contours. Vision research, 49, 2518-2530.

Gibson J. J., Radner, M. (1937). Adaptation, after-effect and contrast in the perception of tilted lines. I. Quantitative studies. Journal of Experimental Psychology, 20(5), 453-467.

Graham N. V. (2011). Beyond multiple pattern analyzers modeled as linear filters (as classical V1 simple cells): useful additions of the last 25 years. Vision Research, 51, 1397-1430.

Held, R., Shattuck-Hufnagel, S. & Moskowitz, A. (1082). Color-contingent tilt aftereffext: spatial frequency specificity. *Vision Research*, 22, 811-817.

Hess, R. F., Doshi, S. (1995). Adaptation to spatial offsets. Perception, 20, 453-467.

Kayaert, G., Biederman, I., Op de Beeck, H. P., & Vogels, R. (2005). Tuning for shape dimensions in macaque inferior temporal cortex. European Journal of Neuroscience, 22, 212-224. doi: 10.1111/j.1460-9568.2005.04202.x

Lee, T. S. & Yuille, A. L. (2007). Efficient Coding of Visual Scenes by Grouping and Segmentation: Theoretical Principles and Biological Evidence. In the Bayesian Brain: Probabilistic Approaches to Neural Coding. Eds. K. Doya, S. Ishii, A. Pouget & R.P.N. Rao. MIT Press. pp 145-188.

Mandelbrot B (1982). The fractal Geometry of Nature. W.H. Freeman & Co.

Morgan M., Mareschal I., Chubb C., Solomon J. (2012). Perceived pattern regularity computed as a summarystatistic: implications for camouflage. Proceedings of the Royal Society,(doi: 10.1098/rspb.2011.2645)

Moulden, B., Kingdom, F. & Gatley, L. F. (1990). The standard deviation of luminance as a metric for contrast in random-dot images. Perception, 1990, 19, 79-101.

Nishida S., Ledgeway T., Edwards M. (1997) Dual multiple-scale processing for motion in the human visual system. Vision Research, 37, 2685-2698.

Oppenheim, A. V. & Lim, J. S. (1981). The importance of phase in signals. Proceedings IEEE, 69, 529-541.

Pasupathy, A., & Connor, C. E. (2001). Shape representation in area V4: Position-specific tuning for boundary conformation. Journal of Neurophysiology, 86(5), 2505-2519.

Piotrowski, L. N. & Campbell, F. W. (1982). A demonstration of the visual importance and flexibility of spatial-frequency amplitude and phase. Perception, 11, 337-346.

Robinson, A. E., Hammon, P. S. & de Sa, V. R. (2007). Explaining brightness illusions using spatial filtering and local response normalization. Vision Research, 47, 1631-1644.

Schofield A. J., Georgeson M. A. (1999) Sensitivity to modulations of luminance and contrast in visual white noise: separate mechanisms with similar behaviour. Vision Research, 39, 2697-2716.

Sutherland S. (1954). Figural after-effects, retinal size and apparent size. Journal of Experimental Psychology, 6, 35-44.

Ware, C. & Mitchell, D. E. (1974). The spatial selectivity of the tilt aftereffect. *Vision Research*, 14, 735-737.

Webster, M.A. (2011). Adaptation and visual coding. Journal of Vision, 11(5):3, 1-23.

Wertheimer M. (1938). “Untersuchungen zur Lehre der Gestalt, II”. Psychologische Forschung 4, pp. 301-350, 1923. Translation published as Laws of Organization in Perceptual Forms, in Ellis, W. (1938). A source book of Gestalt psychology (pp. 71-88). London: Routledge & Kegan Paul.

Whitaker, D., McGraw, P. V., Levi, D. M. (1997). The influence of adaptation on perceived visual location. Vision Research, 37(6), 2207-2216.

Yeh, S., De Valois, R. L., De Valois, K. K., Chen, I. (1991). Adaptation to spatial position. Investigative Ophthalmology and Visual Science, 32, 1268.

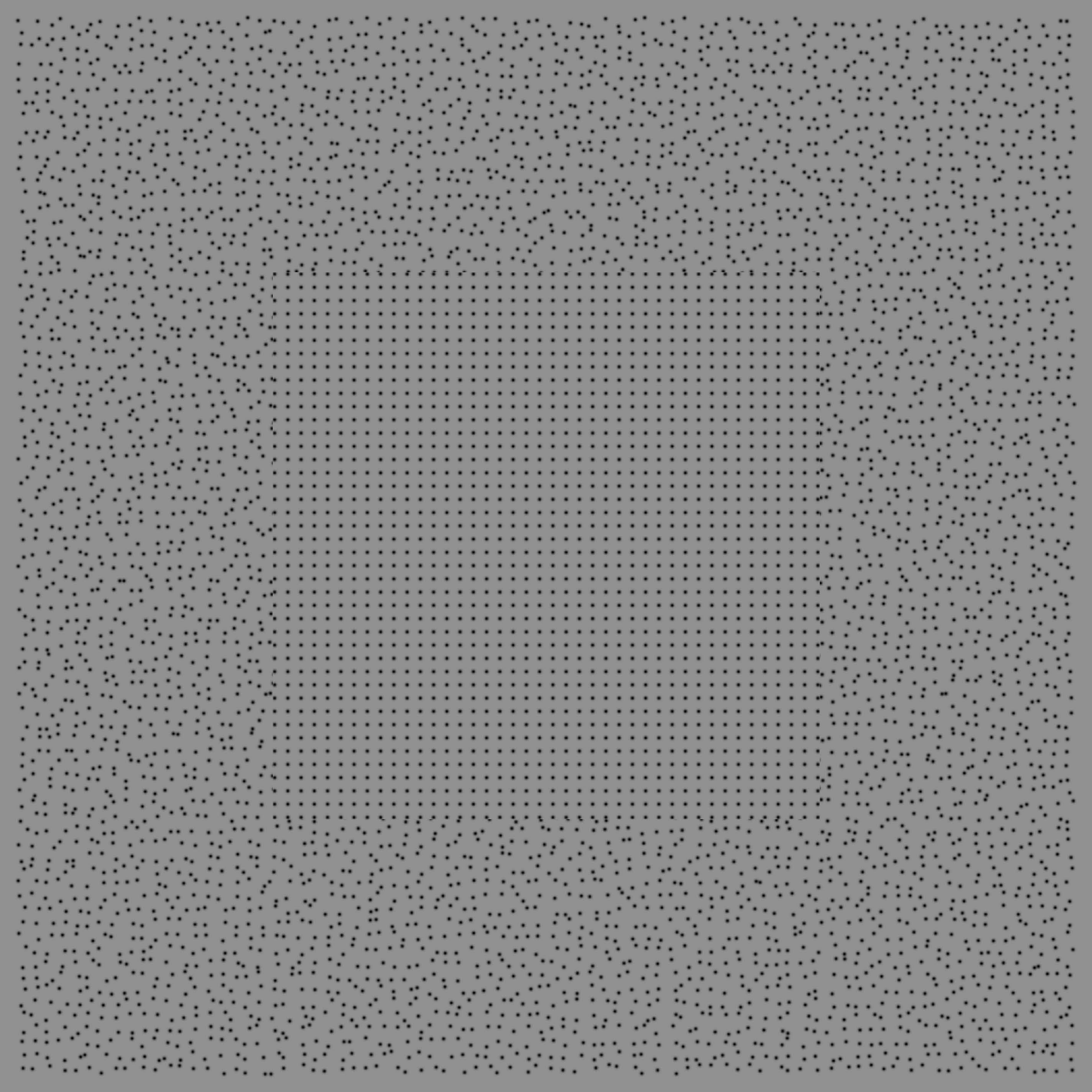

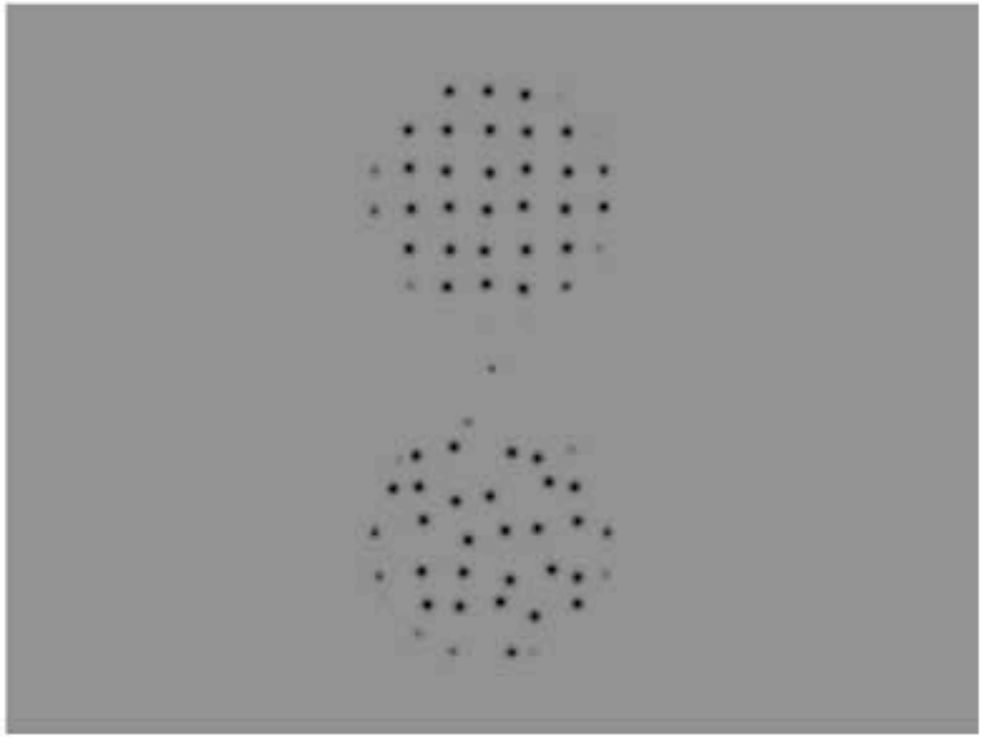

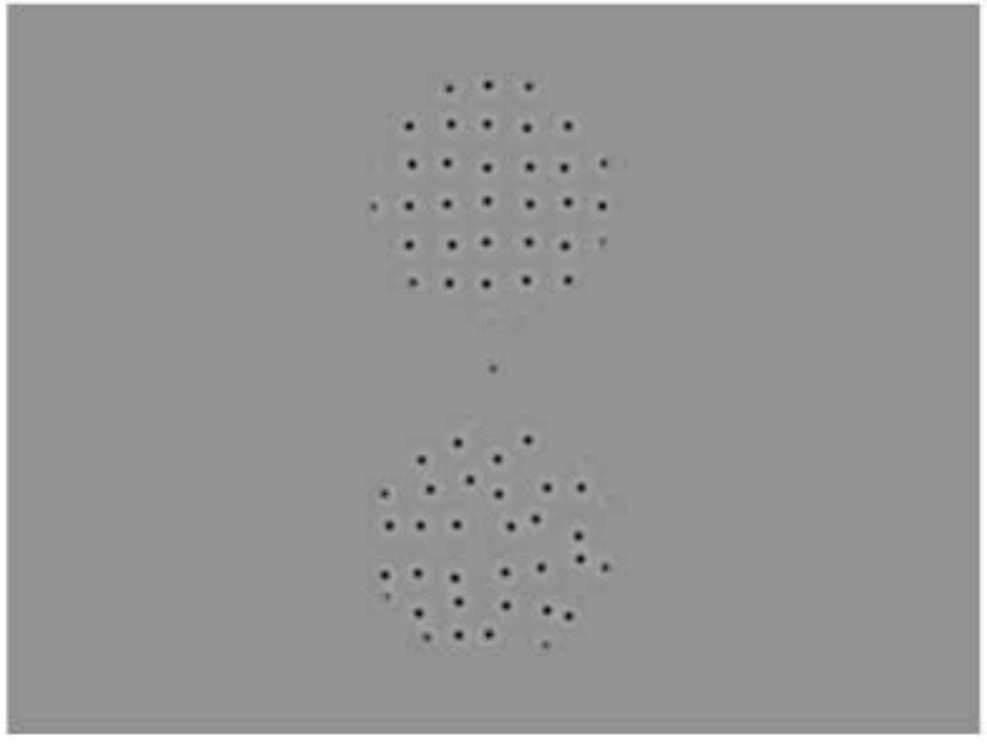

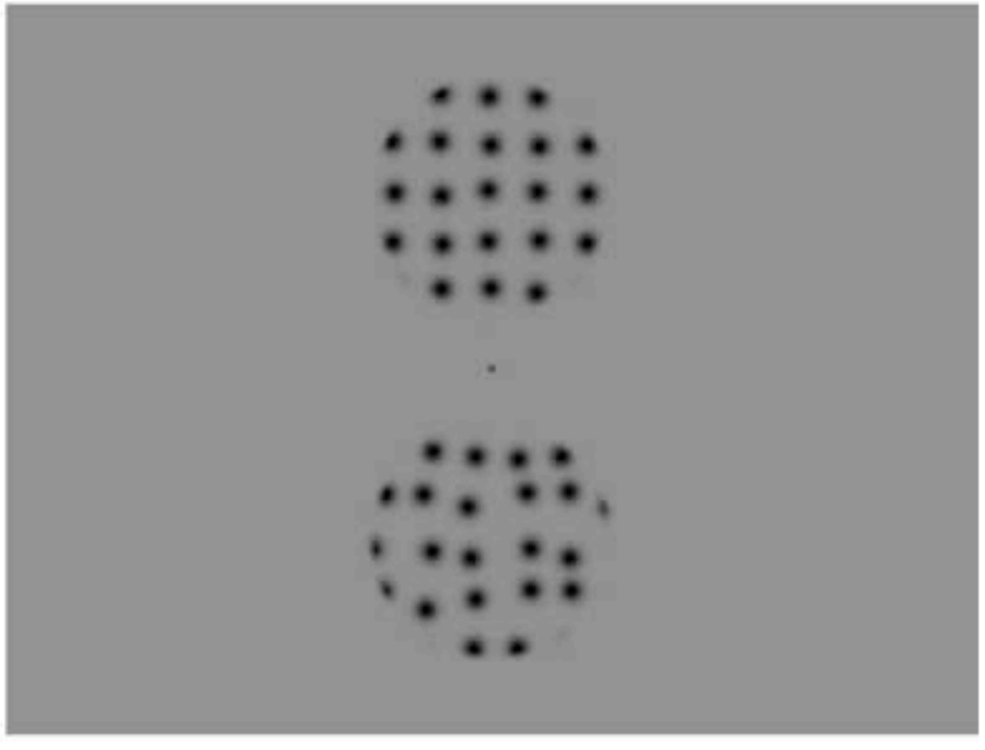

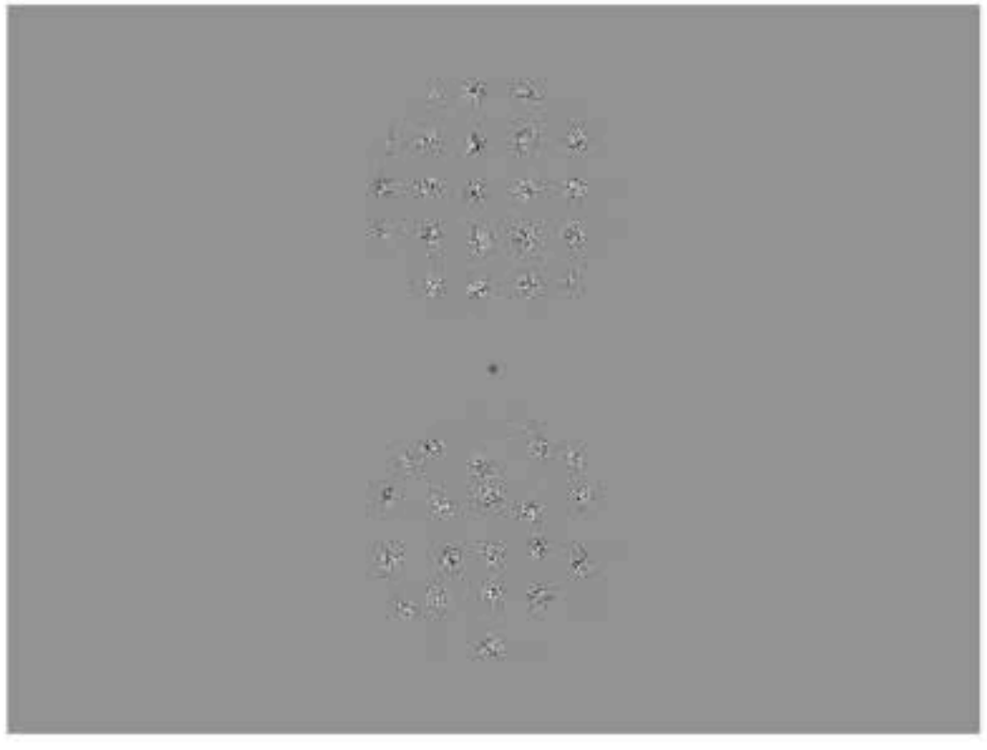

Adaptor

Test

Dual Adaptor

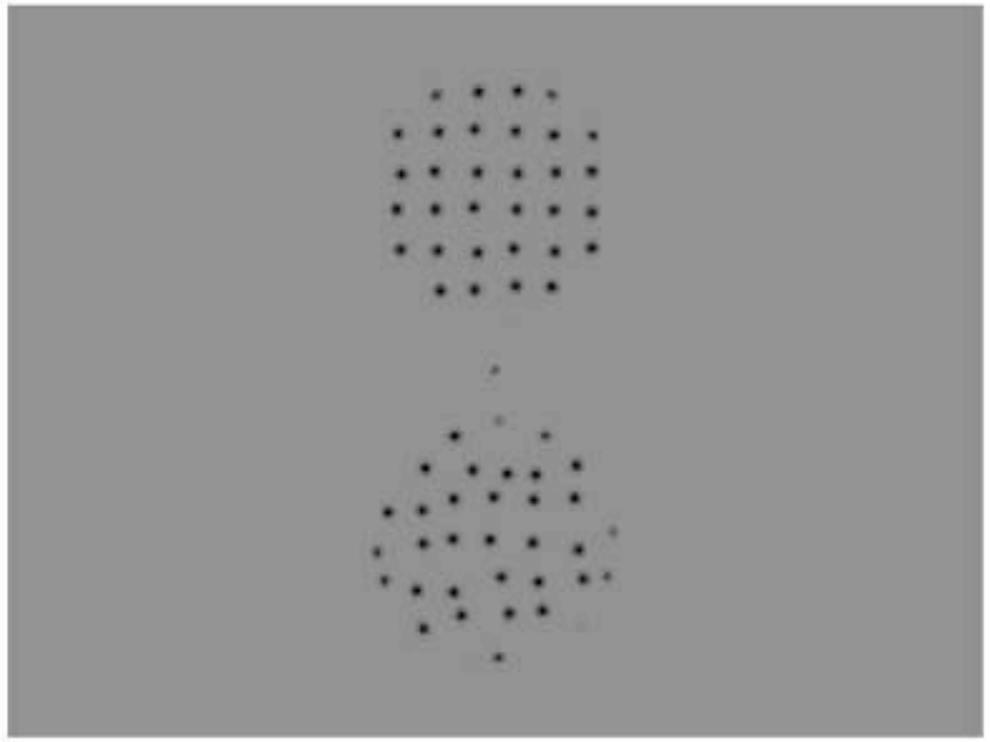

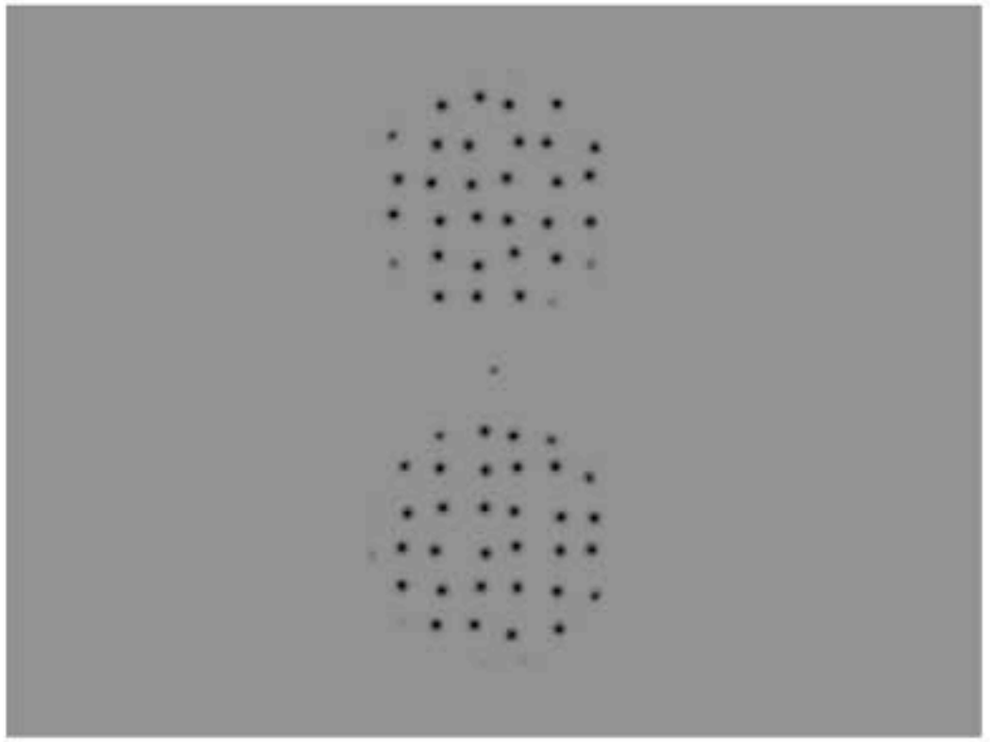

Single Adaptor

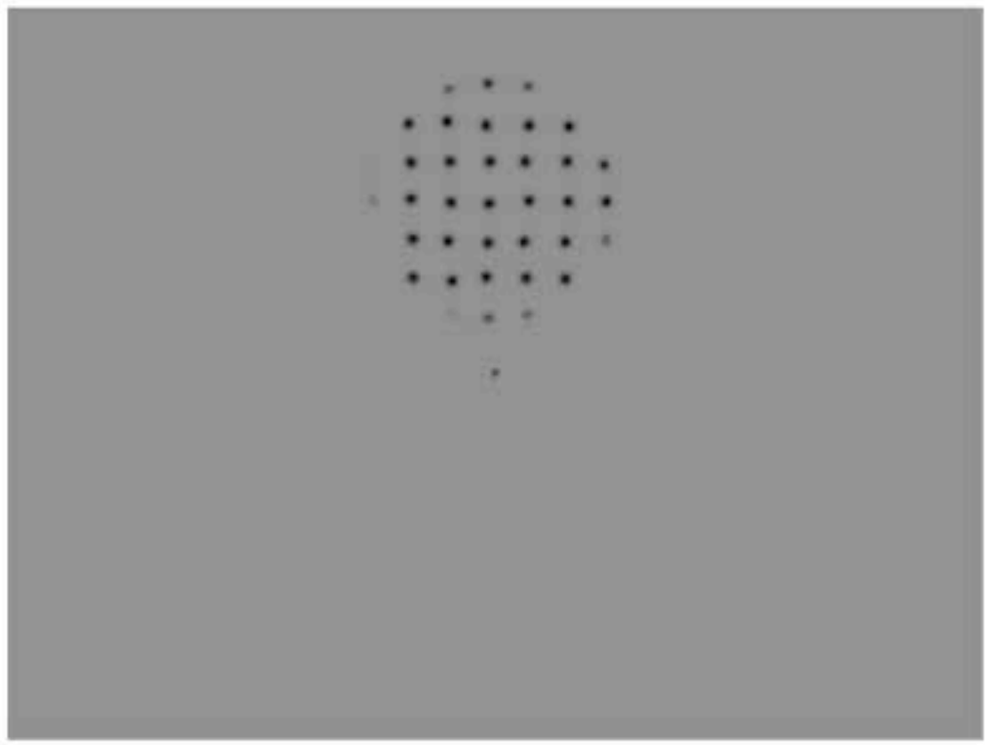

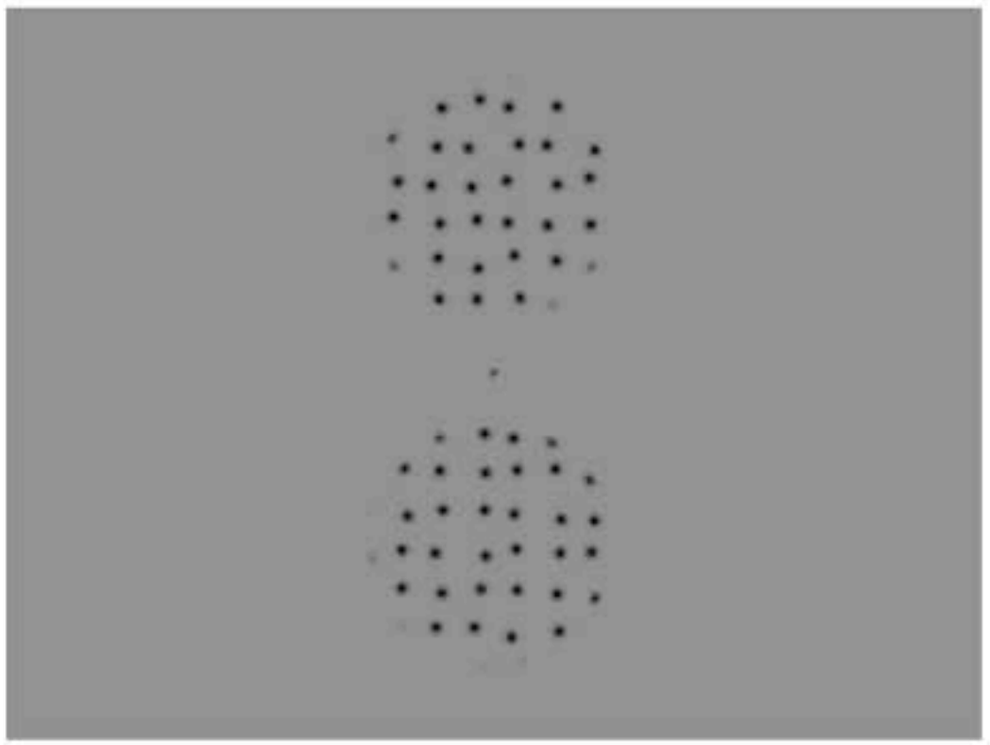

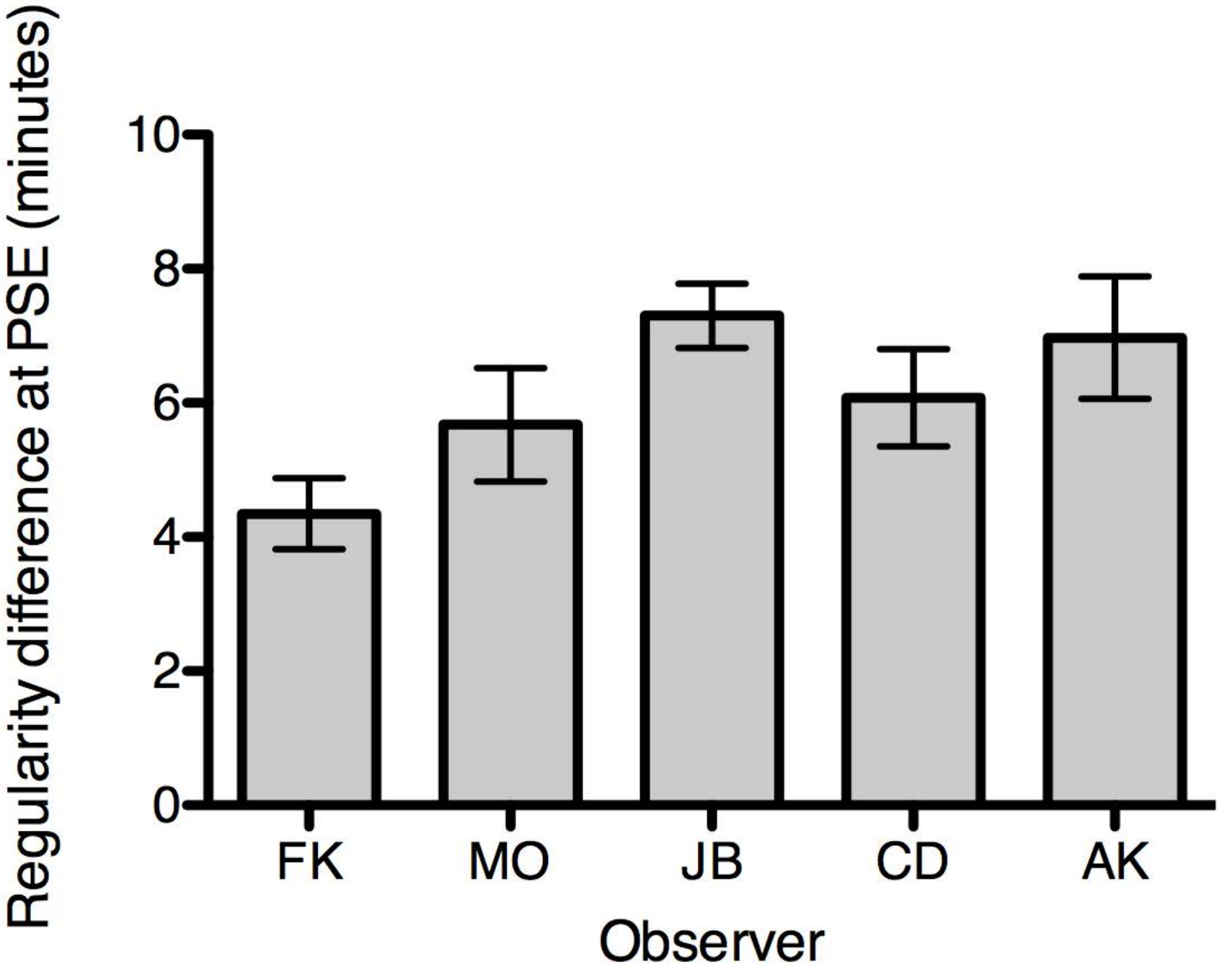
Regularity difference at PSE (minutes)
10
8
6
4
2
0
FK
MO
JB
CD
AK
Observer

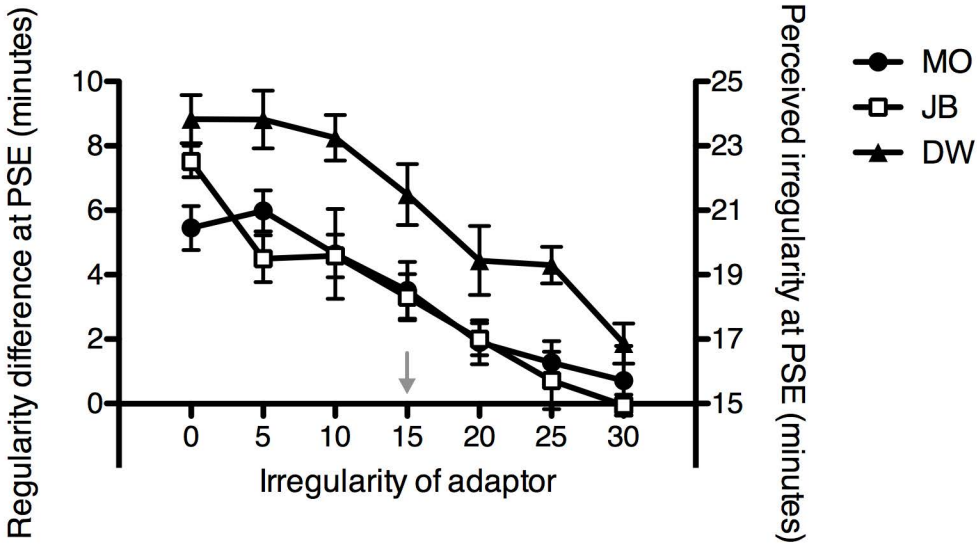
Regularity difference at PSE (minutes)
10
8
6
4
2
0
0
5
10
15
20
25
30
Irregularity of adaptor
25
23
21
19
17
15
Perceived irregularity at PSE (minutes)
MO
JB
DW

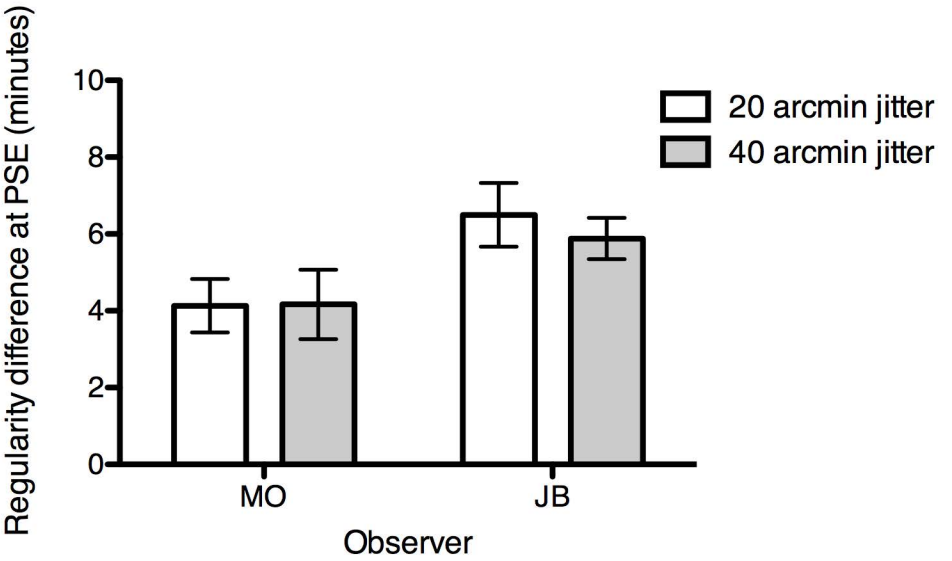
Regularity difference at PSE (minutes)
10
8
6
4
2
0
MO
JB
Observer
20 arcmin jitter
40 arcmin jitter

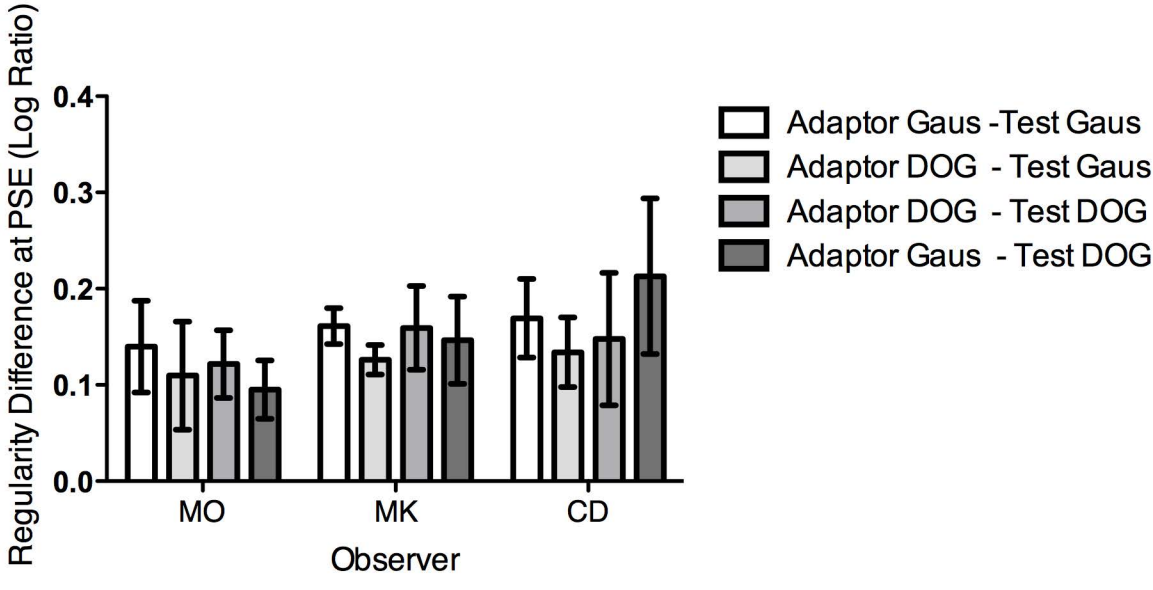
Regularity Difference at PSE (Log Ratio)
0.4
0.3
0.2
0.1
0.0
MO
MK
CD
Observer
Adaptor Gaus -Test Gaus
Adaptor DOG - Test Gaus
Adaptor DOG - Test DOG
Adaptor Gaus - Test DOG

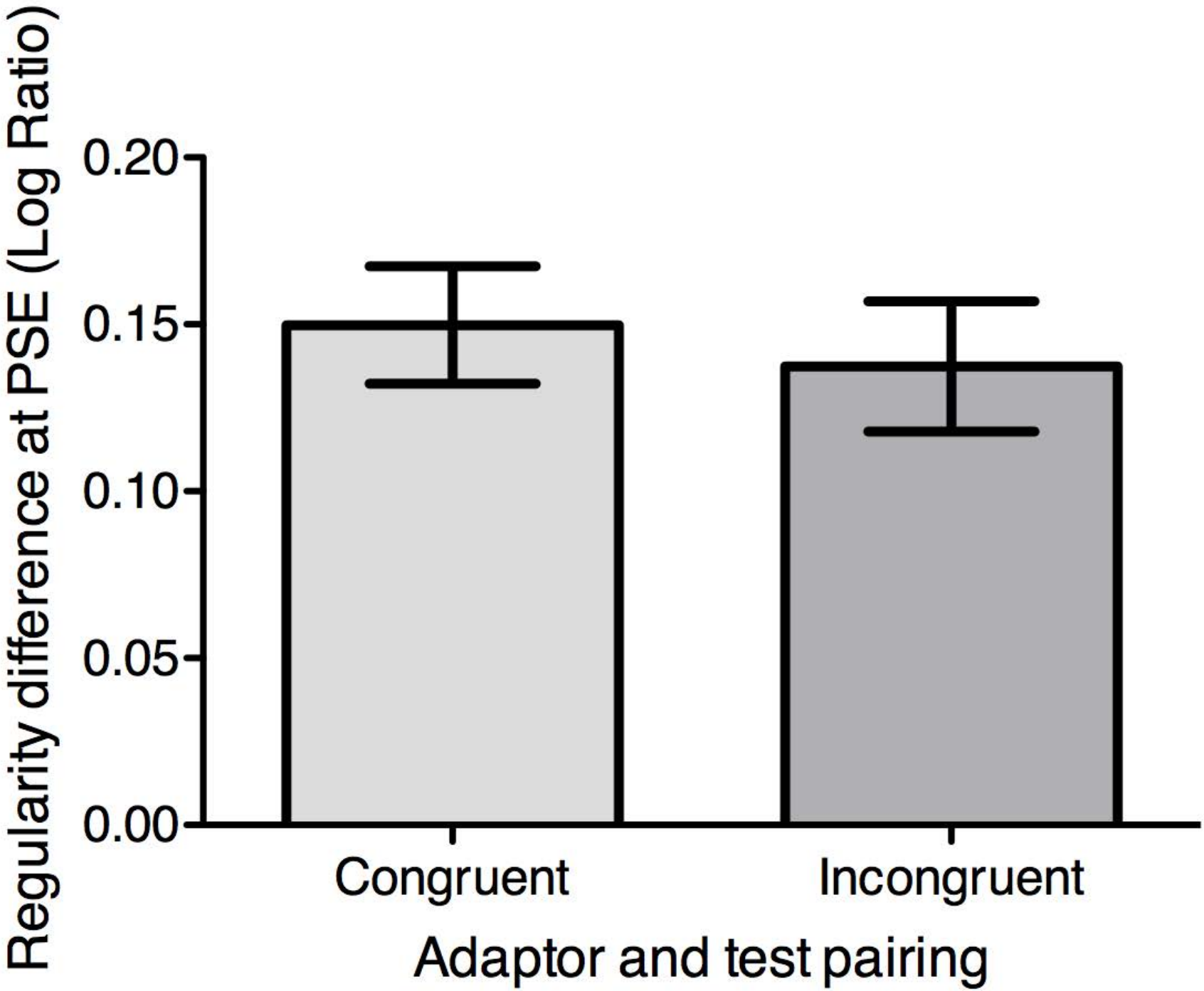
Regularity difference at PSE (Log Ratio)
0.20
0.15
0.10
0.05
0.00
Congruent
Incongruent
Adaptor and test pairing

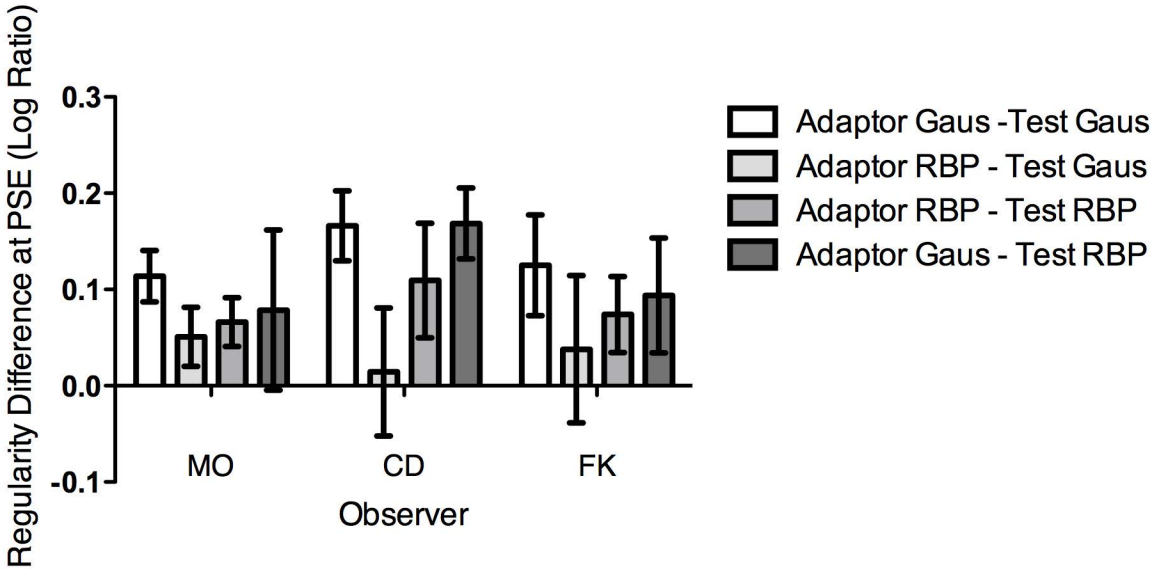
Regularity Difference at PSE (Log Ratio)
0.3
0.2
0.1
0.0
-0.1
MO
CD
FK
Observer
Adaptor Gaus -Test Gaus
Adaptor RBP - Test Gaus
Adaptor RBP - Test RBP
Adaptor Gaus - Test RBP

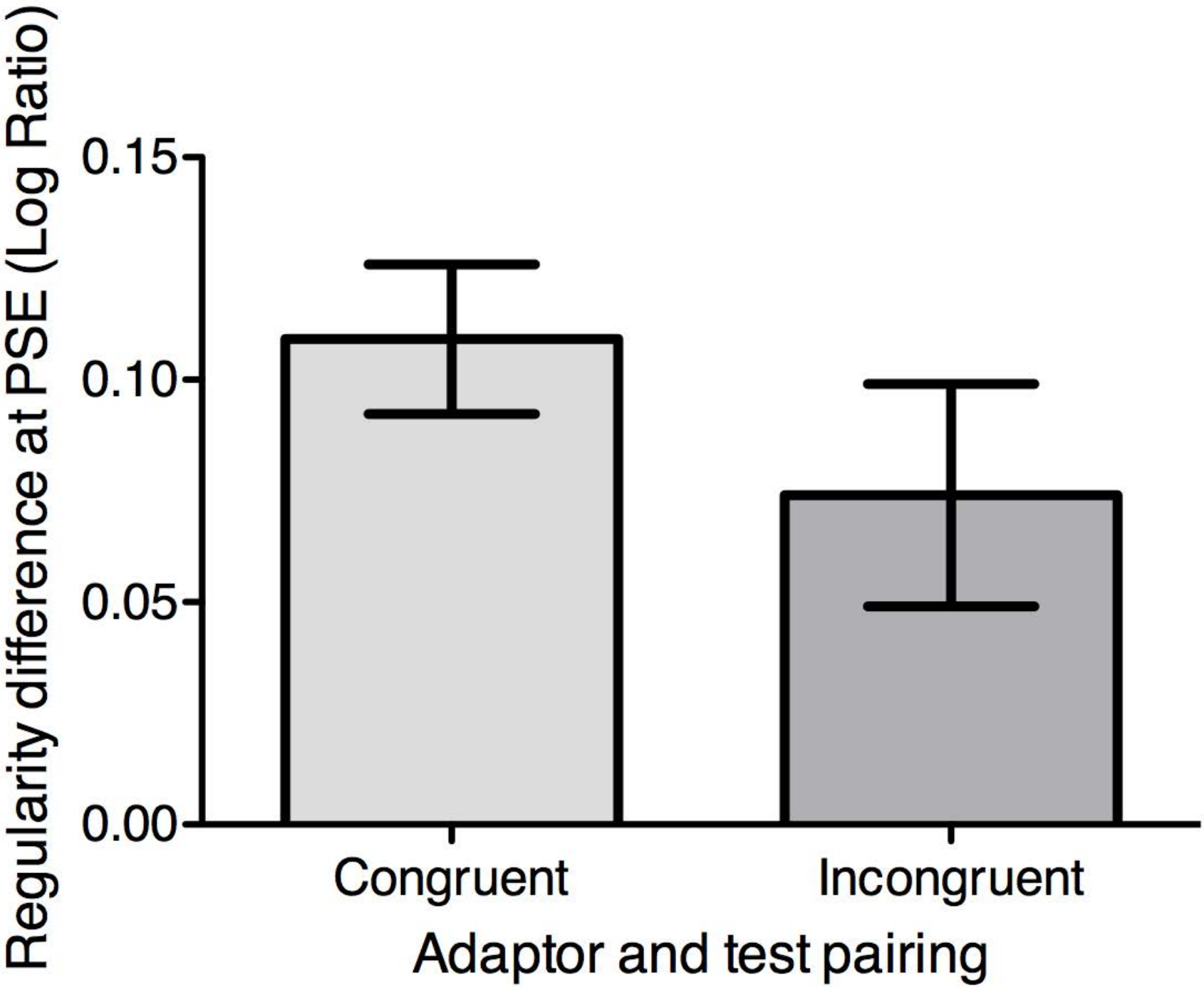
Regularity difference at PSE (Log Ratio)
0.15
0.10
0.05
0.00
Congruent
Incongruent
Adaptor and test pairing

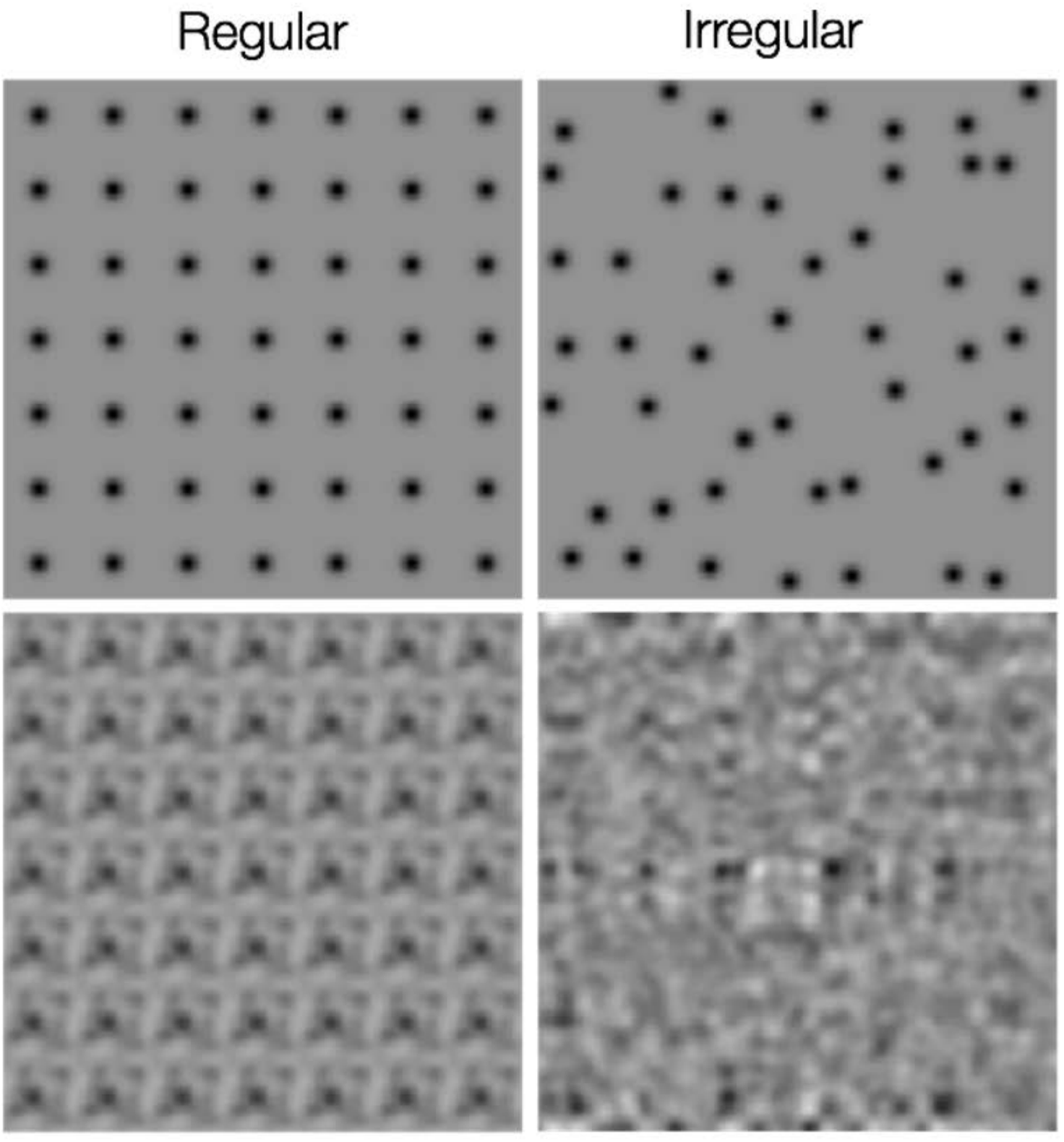
Regular
Irregular
Amplitude regular
Phase irregular
Amplitude irregular
Phase regular

a

1st-stage
Gabor filter

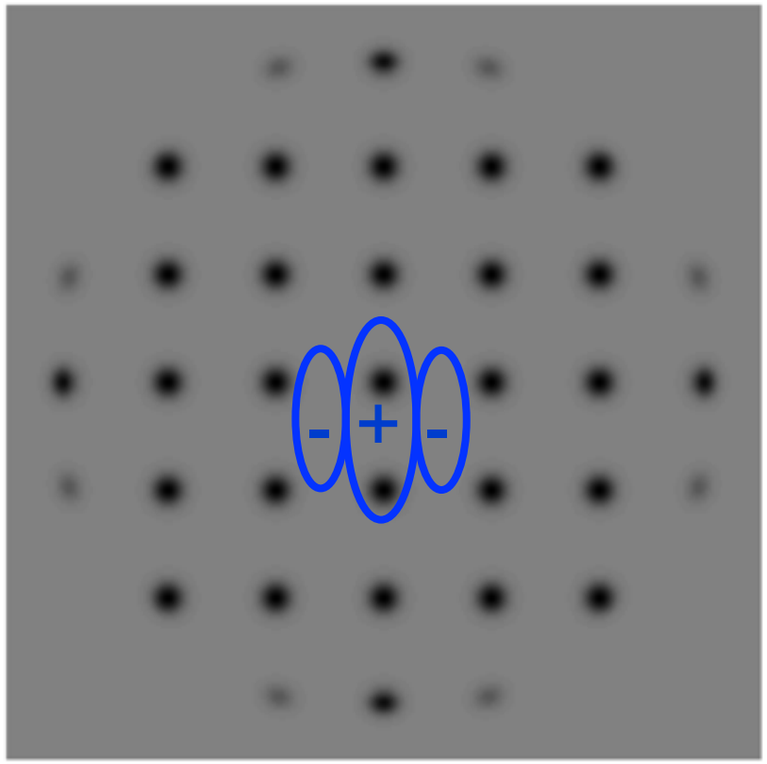

Squaring

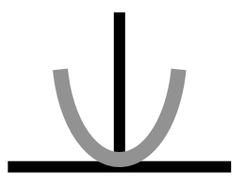

2nd-stage pools
1st-stage outputs

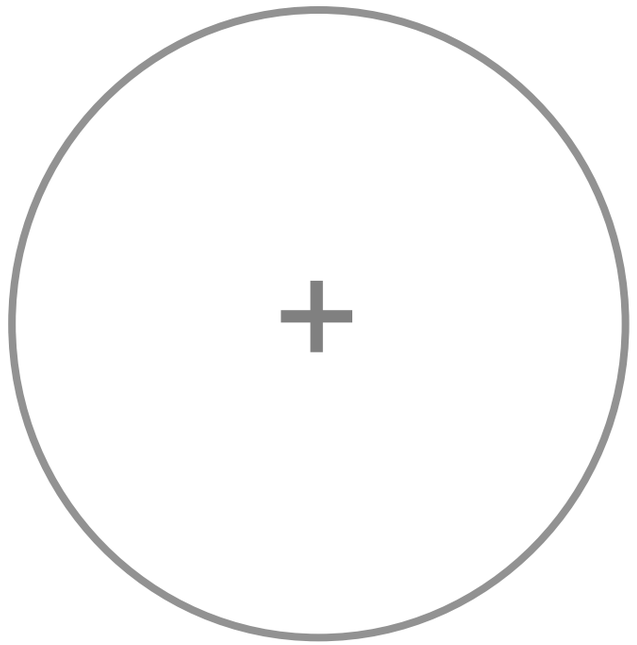

b

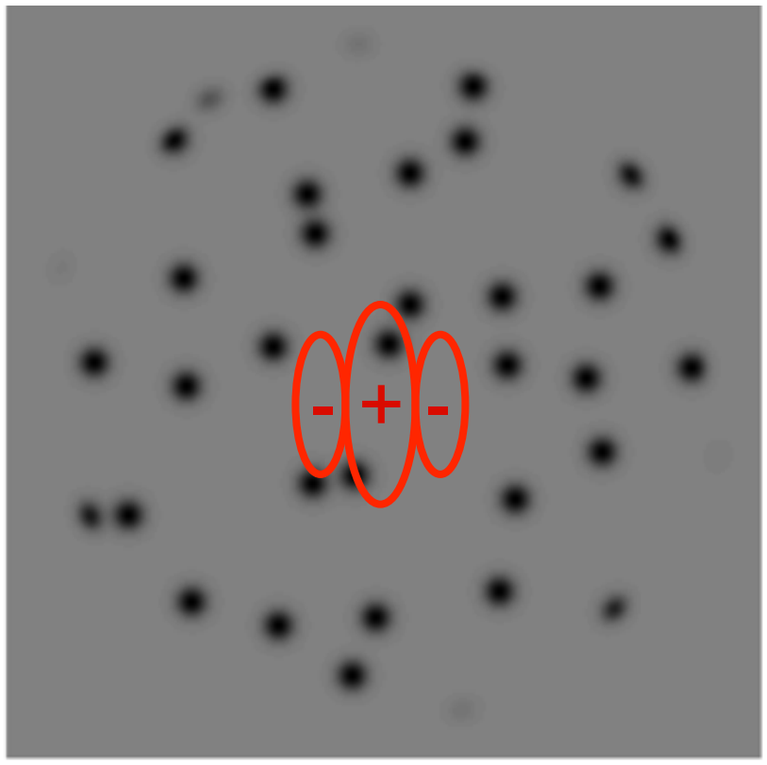

c

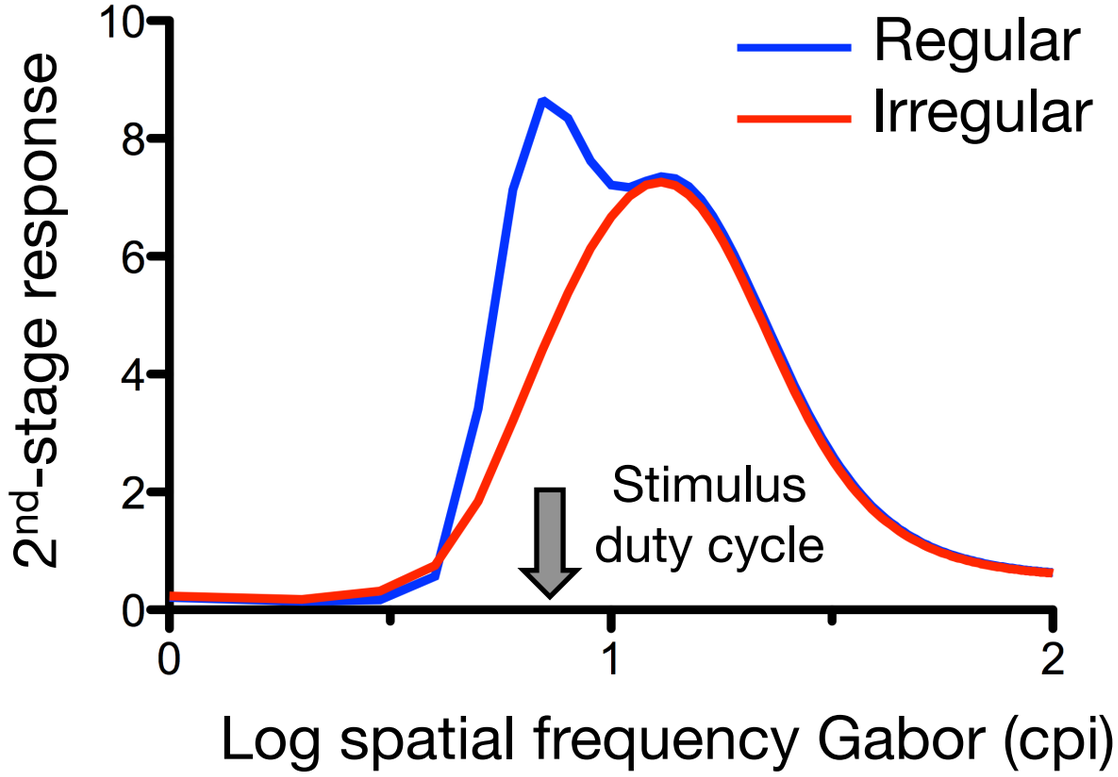

1st-stage
Gabor filter

Squaring

2nd-stage
Gabor filter

Squaring

3rd-stage pools 2nd-
stage responses